ELSEVIER

Materials Science and Engineering A 489 (2008) 439–443

MATERIALS SCIENCE & ENGINEERING A

www.elsevier.com/locate/msea

Short communication

Mechanical properties of a density-graded replicated aluminum foam

Alan H. Brothers, David C. Dunand *

Department of Materials Science and Engineering, Northwestern University, Evanston, IL 60208, USA

Received 13 September 2007; received in revised form 13 November 2007; accepted 26 November 2007

Abstract

The compressive mechanical properties of uniform and density-graded Al-6061 foams, produced by replication of polymer foams, are measured. While the uniform foam shows compressive behavior characteristic of conventional (uniform) metallic foams with a near constant plateau stress, the density-graded foam exhibits a smoothly rising plateau stress. This behavior is modeled using a simple series composite model based on semi-empirical scaling relationships for the compressive behavior of uniform foams.

Keywords: Liquid infiltration; Radiography; Functionally graded materials; Modeling; Density gradient

Functionally graded materials optimize performance through controlled property gradients [1], an approach that can be extended to metal foams having graded relative density. The first to do so was Neubrand [2], who used electrochemical methods to create Cu and W foams with continuously graded relative densities (defined as ρ/ρ_s, where ρ is the foam density and ρ_s is the density of the solid metal) in the range of 10–70%. Continously graded Al foams were produced by Matsumoto et al. [3], who used graded chemical dissolution to achieve $\rho/\rho_s = 5$–10%. Stepwise-graded Ni foams have been produced by powder compaction with placeholders (layer densities 30–70%) [4], and with a pulse-current-assisted sintering method [5], and stepwise-graded Cu ($\rho/\rho_s = 30$–50%) via sintering of fibrous preforms [6]. Mortensen and co-workers layered aluminum foams, made by replication of soluble NaCl placeholders [7,8], to create sandwiches with core relative densities $\rho/\rho_s = 15$–45%. They also showed that density-grading offers little or no advantage for stiffness-limited beams, but does offer a weight reduction for certain strength-limited applications [8].

The processing method used here is based on investment-casting replication of polymeric precursors which have been density-graded by non-uniform compression. The method, described in detail previously [9], is distinctive for its capacity to create continuous, complex, macroscopic density profiles. Reticulated open-cell polyurethane foam with a measured mean pore size of 2.1 mm and mean relative density 2.7% (Foamcraft, Inc., Skokie, IL, USA) was used as the precursor. One sample (hereafter, the uniform-density sample) was processed from a right circular cylinder (diameter 16 mm, height 18 mm) of precursor, and a second sample (hereafter, the density-graded foam) from a truncated cone (minimum diameter 16 mm, maximum diameter 22.6 mm, height 21 mm). Both precursors were dip-coated with plaster wetting agent (Rio, Albuquerque, NM, USA), inserted into quartz tubes of inner diameter 16 mm (oil-lubricated to minimize friction), and invested with casting plaster (Satin Cast 20, Kerr Lab, Albuquerque, NM, USA). After overnight plaster setting, precursors were pyrolyzed by heating in freely convective air at a rate of 2 K/min to a temperature of 773 K, soaked for 4–6 h, and freely cooled. The resulting molds were pressure-infiltrated in graphite-coated quartz crucibles by molten Al-6061 at 973 ± 5 K, using an argon gas overpressure of 3.5 kPa. To remove the plaster investment, samples were repeatedly soaked at 573 K for 10 min intervals and then water quenched, with water jet rinsing between cycles to remove loosened plaster. After this, a final cleaning was done ultrasonically in water. Samples were then machined into cylinders using electric discharge machining, to eliminate surface defects associated with processing and handling and to ensure flat and parallel surfaces for testing. Final dimensions were 12.8 mm diameter and 14.7 mm height for the uniform-density standard, and 13.7 mm diameter and 15.4 mm height for the density-graded sample. Following machining, both samples were heat treated to an optimally aged (T6) condition.

Net sample densities were determined by measuring dry mass and dimensions, and both samples were analyzed for rela-

* Corresponding author. Tel.: +1 847 491 5370; fax: +1 847 491 7820.
E-mail address: dunand@northwestern.edu (D.C. Dunand).

0921-5093/$ – see front matter © 2007 Elsevier B.V. All rights reserved.
doi:10.1016/j.msea.2007.11.076

tive density radiographically, by rotating each specimen (with a period of 0.3 s) about its gauge axis, while taking a radiographic image (exposure time 480 s) using a white X-ray source operating at 25 kV and 20 mA. The images were then analyzed digitally to recover the relative density profiles via the absorption equation and a foil standard, as described previously [9]. Some data (near where the samples were mounted to the rotating stage) were lost, so the calculated profiles are slightly shorter than the true sample heights. Compressive mechanical properties were measured for both specimens during quasistatic uniaxial compression at a nominal strain rate of 10^{-3} s^{-1}.

The compressive mechanical properties of the non-uniform foam are modeled using an isostress composite model. The foam specimen is represented as a stack of N independent layers i, each having uniform density ρ_i, connected in series along the compression axis. Each layer of thickness x_i, represents a single plane of pores of size d, since it would be unphysical to apply a constitutive model to a layer whose dimension accommodates less than one full pore. It follows that the number of layers is equal to the ratio of the specimen gauge length h to pore size, i.e. $N = h/d$. For the present specimen, the value of N is 8.

Initial layer densities ρ_i were assigned based on experimental X-ray data, as described above. As this measurement method averages out individual pores in the radiographs, density data were binned into N points in order to populate the initial layer densities. For each layer, a compressive stress–strain behavior was assigned by extrapolating from a standard specimen with a low and uniform density ρ_o, via the semi-empirical Gibson–Ashby equation for strength in open-cell foams [10]. According to this equation, the ratio of compressive yield strengths between the foam and the solid metal, $\sigma_y/\sigma_{y,s}$, is given by:

$$\frac{\sigma_y}{\sigma_{y,s}} = C\left(\frac{\rho}{\rho_s}^n\right). \quad (1)$$

where C is the 'knockdown factor' and n is the scaling exponent, taking values of $C = 0.3$ and $n = 1.5$ based on best fit for foams of many different densities and structures [10]. At higher strains, this relationship was assumed to hold, and therefore the flow stress $\sigma_i(\varepsilon_i)$ at a strain of ε_i in a layer with density ρ_i could be calculated by $\sigma_i(\varepsilon_i) = \sigma_o(\varepsilon_i)\ (\rho_i/\rho_o)^n$, where $\sigma_o(\varepsilon_i)$ represents the flow stress of the low-density standard at the same uniaxial strain, ε_i. When the stress–strain behavior of each layer had been extrapolated in this fashion, the model composite was subjected to an incrementally increasing applied stress σ. For each value of σ, the corresponding strains ε_i produced within each layer were computed and summed to determine the total (macroscopic) foam strain ε. This process was repeated to generate a stress–strain curve for the density-graded foam, given only its initial relative density profile ρ_i and the behavior of the uniform-density standard $\sigma_o(\varepsilon_i)$.

Scanning electron micrographs illustrating the structure of the polyurethane foam precursor are shown in Fig. 1a and b. The precursor generally consists of nearly straight struts of roughly triangular cross-section. Also visible are a cell wall which partially survived the reticulation process (Fig. 1a) and some surface ripples (Fig. 1b). This basic precursor structure was faithfully replicated in the metallic foam; there are, however, plaster deposits on many strut surfaces. Images showing two replicated Al struts, one with almost no retained plaster deposits, and the other with significant deposits, are shown in Fig. 1c and d, respectively. While some such deposits were found previously in replicated foams with larger (ca. 5 mm) pores [9],

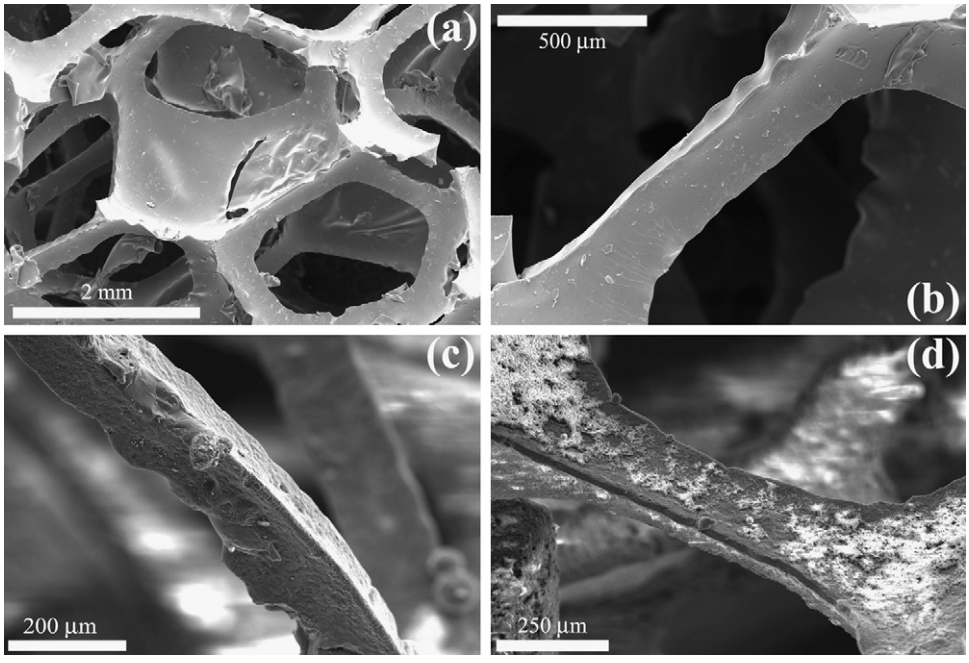

Fig. 1. Scanning electron micrographs showing: (a) precursor pore structure, including one partially ruptured cell wall; (b) a characteristic undeformed precursor strut; (c) an Al foam strut, bearing no retained plaster; and (d) an Al foam strut with retained plaster deposits.

the deposits here were more significant in size and number, due to more restricted access of the water used for plaster removal and rinsing, and a higher number of partially intact cell walls in the precursor (Fig. 1a).

Fig. 2 shows the radiographically determined relative density profile of each sample. Both foams show large local density fluctuations, resulting from the small sample dimension/pore size ratio, but the uniform foam lacks any overall gradient, unlike the density-graded foam. The average relative densities calculated from these profiles were 3.4% for the uniform-density foam, and 6.3% for the density-graded foam, compared to $3.0 \pm 0.1\%$ and $5.5 \pm 0.2\%$, respectively, based on mass and dimensions. The larger density error for the graded specimen is likely due to its higher amount of retained plaster, as discussed in the previous paragraph.

Compressive stress–strain curves for the two samples are shown in Fig. 3a. The uniform-density foam shows conventional metallic foam behavior, with an extended and nearly flat plateau region followed by densification at high strain. By contrast, the density-graded sample shows a pronounced positive slope in the plateau region, consistent with deformation beginning in the lowest-density region of the sample and progressing towards the stronger, higher-density regions. Also shown in Fig. 3a is the prediction of the series model, taking as inputs the stress–strain

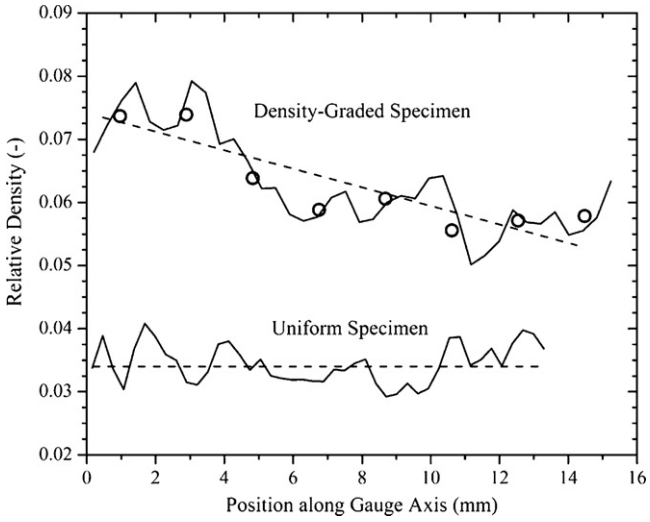

Fig. 2. Radiographic relative density profiles of the uniform and density-graded foams. The data have not been binned, but the binned data (i.e., the initial layer densities used in modeling) are shown as open circles. The dashed lines are provided as visual guides only.

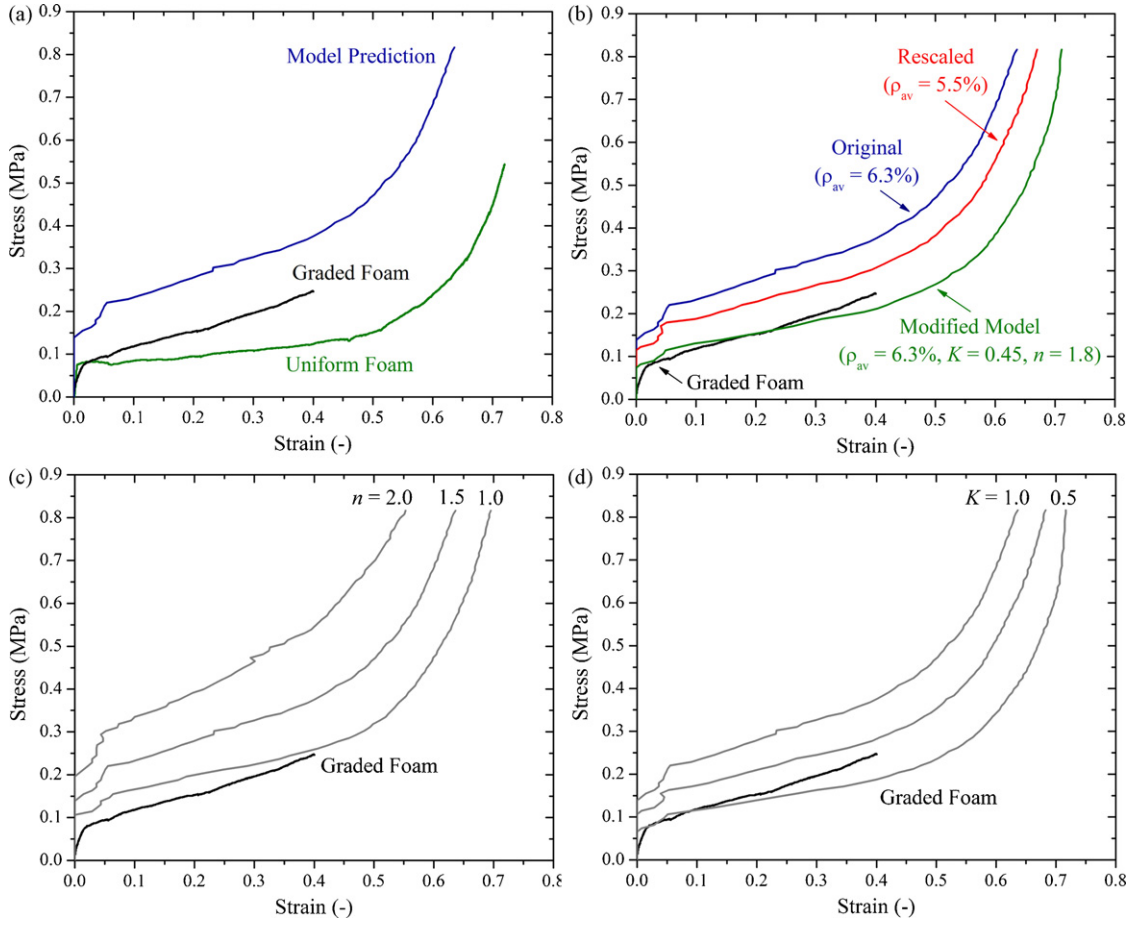

Fig. 3. Measured and predicted compressive stress–strain curves. (a) Measured curves of the uniform and density-graded foams, and predicted curve using Eq. (1) with $K = 1.0$ and $n = 1.5$. (b) Effect of rescaling the foam density profile to rectify differences in measured net density ("Rescaled"). Also shown is the model prediction with $K = 0.45$ and $n = 1.8$ ("Modified Model"). (c) Variation of n, with a constant $K = 1.0$. (d) Variation of K, with a constant $n = 1.5$.

curve and net radiographic density (3.4%) of the uniform-density foam, and the relative density profile of the density-graded sample (Fig. 2). The positive slope of the plateau region is correctly predicted by the model, which however overestimates the actual flow stress throughout the whole strain range. It is noted that, in this and subsequent model predictions, the lack of explicit elasticity in the model makes it appear as though the graded foam shows no deformation until yield.

One possible explanation for the discrepancy between measured and predicted stress–strain behavior is uncertainty in the sample density due to residual plaster (Fig. 1d). On the assumption that the error in radiographic and direct density measurements comes from residual plaster, and that this plaster carries no load, it is possible to rescale the density profile of the graded foam so that its average value (6.3%) corresponds to the average density measured by mass and dimensions (5.5%). Applying the model in this case yields the curve labeled "Rescaled" in Fig. 3b, partially but not fully eliminating the discrepancy. Given that the properties of a metal foam are usually very well determined by its relative density and the properties of its base alloy (in this case, the foams have identical base alloys), it seems likely that the largest part of the observed discrepancy can be found in the structure of the model itself.

A number of assumptions are implicit in this simple model. First is the conventional assumption that individual layers are non-interacting, i.e., that the strain in any layer is independent of the strains in neighboring layers. It is often observed that non-graded foam materials collapse along a single, or small number of, crush bands [10]. Within such a band, local strains are very high, while the surrounding foam remains largely undeformed until the material in the band densifies. At that point the band extends to engulf those neighboring regions, where the process is repeated. Such a picture is consistent with the assumption of non-interacting layers in a graded foam, barring any significant axial variations in the extent of lateral contraction (e.g., auxetic behavior [11]) resulting from the curved or buckled struts comprising the deformed regions of the precursor [9].

Secondly, there is the assumption that Eq. (1) may be used to directly scale flow stresses at strains past macroscopic yield. In general terms, this is not justified, since it is known that the stress–strain curves of high-density foams differ qualitatively from those of low-density foams (the latter generally show flatter plateau regions and later densification [12]). However, the model is applied here only to layers with low relative densities, and with only modest density differences between layers. It is therefore believed that the errors induced via this assumption are minimal, at least until large strains.

Lastly, there is the assumption is that Eq. (1) may be used to predict the behavior of layers of various relative densities. This equation is known to be broadly applicable to foams, but deviations can be expected when the foam structure is qualitatively different at different relative densities. Due to the fact that all but the lowest-density regions have significantly deformed struts, this seems the most likely source of error. Several specific possibilities must therefore be considered.

First among these is the possibility that the assumed scaling exponent $n = 1.5$ (Eq. (1)) does not apply to the graded foam. The effect of changes in this exponent is illustrated by the additional model curves shown in Fig. 3c, representing values of n between 1 and 2. Changing n shifts both the magnitude of the stress, and the slope of the plateau region. It is also possible that there are differences in the knockdown factor C in Eq. (1) representing each layer. This coefficient is often interpreted as a measure of the 'efficiency' of the foam structure, and/or the concentration and severity of flaws therein, with lower values representing weaker foams for a given density. It is plausible that the high-density regions of the graded sample, replicated from the buckled and twisted struts in the compressed elastomeric precursor, are less mechanically efficient than the straighter struts of the low-density regions. It has also been shown previously that microstructural flaws such as replicated air bubbles in the investment are more prevalent in the high-density regions [9]. Either case would lead to a decrease in the knockdown coefficient of the high-density regions relative to the low-density, such that the ratio of flow stresses for these regions could be given by:

$$\sigma_i(\varepsilon_i) = K\sigma_o(\varepsilon_i)\left(\frac{\rho_i}{\rho_o}\right)^{1.5}, \quad (2)$$

where K is the ratio of knockdown factors, $C_i/C_o < 1$. The effect of variation in K is shown by the model curves in Fig. 3d. Values of K near 0.5 lower the numerical discrepancy between measured and model curves, but do so at the expense of the good correlation in plateau-region slope.

Finally, simultaneously modifying both K and n (to values of 0.45 and 1.8, respectively) brings the model prediction into reasonable agreement with the experimental data, as indicated by the plot labeled "Modified Model" in Fig. 3b. This is not to suggest that these values are truly representative of the graded foam behavior, as more experimental data would be needed to probe the true properties of these structures. Rather, it shows that, within the reasonable limits of the parameters of Eq. (1), the behavior of a density-graded foam stressed uniaxially parallel to its density gradient can be adequately approximated, and therefore that simple and conventional scaling laws, in combination with series composite models, are a plausible approach to understanding the mechanical properties of density-graded foams.

Acknowledgements

This work was performed under the auspices of the U.S. Department of Energy via the University of California, Lawrence Livermore National Laboratory under Contract W-7405-Eng-48. The authors thank Dr. A.M. Hodge for management and support, Foamcraft, Inc. for providing precursors, and Suzie Schnepp (Art Institute of Chicago) for invaluable help in collecting radiographic data.

References

[1] A. Mortensen, S. Suresh, Int. Mater. Rev. 40 (1995) 239.
[2] A. Neubrand, J. Appl. Electrochem. 28 (1998) 1179.
[3] Y. Matsumoto, A.H. Brothers, S.R. Stock, D.C. Dunand, Mater. Sci. Eng. A 447 (2007) 150.

[4] C. Solaiyan, P. Gopalakrishnan, S. Dheenadayalan, I.A. Raj, S. Muzhumathi, R. Chandrasekaran, R. Pattabiraman, Indian J. Chem. Tech. 6 (1999) 48.
[5] Z. Song, S. Kishimoto, N. Shinya, Adv. Eng. Mater. 6 (2004) 211.
[6] H. Togashi, K. Yuki, H. Hashizume, Fusion Sci. Technol. 47 (2005) 740.
[7] A. Pollien, Y. Conde, L. Pambaguian, A. Mortensen, Mater. Sci. Eng. A404 (2005) 9.
[8] Y. Conde, A. Pollien, A. Mortensen, Scr. Mater. 54 (2006) 539.
[9] A.H. Brothers, D.C. Dunand, Adv. Eng. Mater. 8 (2006) 805.
[10] L.J. Gibson, M.F. Ashby, Cellular Solids: Structure and Properties, second ed., Cambridge University Press, Cambridge, 1997.
[11] J.N. Grima, R. Gatt, N. Ravirala, A. Alderson, K.E. Evans, Mater. Sci. Eng. A 423 (2006) 214.
[12] M.F. Ashby, A.G. Evans, N.A. Fleck, L.J. Gibson, J.W. Hutchinson, H.N.G. Wadley, Metal Foams: A Design Guide, Butterworth-Heinemann, Boston, 2000.